Monthly Notices
of the
ROYAL ASTRONOMICAL SOCIETY

Mon. Not. R. Astron. Soc. **424,** 217–223 (2012) doi:10.1111/j.1365-2966.2012.21185.x

On the determination of the spin of the black hole in Cyg X-1 from X-ray reflection spectra

A. C. Fabian,[1⋆] D. R. Wilkins,[1] J. M. Miller,[2] R. C. Reis,[2] C. S. Reynolds,[3] E. M. Cackett,[1,4] M. A. Nowak,[5] G. G. Pooley,[6] K. Pottschmidt,[7,8] J. S. Sanders,[1] R. R. Ross[9] and J. Wilms[10]

[1]*Institute of Astronomy, Madingley Road, Cambridge CB3 0HA*
[2]*Department of Astronomy, University of Michigan, Ann Arbor, MI 48109, USA*
[3]*Department of Astronomy, University of Maryland, College Park, MD 20742, USA*
[4]*Department of Physics and Astronomy, Wayne State University, Detroit, MI 48201, USA*
[5]*Kavli Institute for Astrophysics and Space Research, MIT, 77 Massachusetts Avenue, Cambridge, MA 02139, USA*
[6]*Cavendish Laboratory, University of Cambridge, JJ Thomson Avenue, Cambridge CB3 0HE*
[7]*CRESST and NASA Goddard Space Flight Center, Code 661, Greenbelt, MD 20771, USA*
[8]*Center for Space Sciemce and Technology, University of Maryland Baltimore County, 1000 Hilltop Circle, Baltimore, MD 21250, USA*
[9]*Physics Department, College of the Holy Cross, Worcester, MA 01610, USA*
[10]*Dr Karl-Remeis-Sternwarte and Erlangen Center for Astroparticle Physics, Sternwartstr. 7, 96049 Bamberg, Germany*

Accepted 2012 April 25. Received 2012 April 16; in original form 2012 February 16

ABSTRACT

The spin of Cygnus X-1 is measured by fitting reflection models to *Suzaku* data covering the energy band 0.9–400 keV. The inner radius of the accretion disc is found to lie within 2 gravitational radii ($r_g = GM/c^2$), and a value of $0.97^{+0.014}_{-0.02}$ is obtained for the dimensionless black hole spin. This agrees with recent measurements using the continuum fitting method by Gou et al. and of the broad iron line by Duro et al. The disc inclination is measured at $23.^{\circ}7^{+6.7}_{-5.4}$, which is consistent with the recent optical measurement of the binary system inclination by Orosz et al. of $27^{\circ} \pm 0.^{\circ}8$. We pay special attention to the emissivity profile caused by irradiation of the inner disc by the hard power-law source. The X-ray observations and simulations show that the index q of that profile deviates from the commonly used, Newtonian, value of 3 within $3r_g$, steepening considerably within $2r_g$, as expected in the strong gravity regime.

Key words: accretion, accretion discs – black hole physics – line: profiles – X-rays: general.

1 INTRODUCTION

Astrophysical black holes are characterized just by mass and spin. The measurement of spin requires observations which probe the immediate environment of the black hole event horizon. Two methods which have emerged using current X-ray observations of luminous accreting black holes rely on fitting either the shape of the reflection component of the spectrum including a broad iron line or the shape and the flux of the quasi-blackbody continuum. Both assume that the accretion disc extends into the innermost stable circular orbit (ISCO), the radius of which is determined by the black hole spin. The reflection fitting method essentially measures the largest gravitational redshift of the disc, which comes from the ISCO, and yields that radius in units of gravitational radii ($r_g = GM/c^2$). The continuum fitting method measures the area of the inner disc and obtains the radius of the ISCO in km. Here we apply the reflection method to *Suzaku* X-ray data of the first stellar mass black hole, Cyg X-1.

Early attempts to measure the spin parameter of Cyg X-1 using the reflection method led to inconsistent results (Miller et al. 2005, 2009). Adopting a Newtonian emissivity profile (surface flux on the disc varies with radius r as r^{-q}, with $q = 3$) and using a special timing mode of *XMM*, a recent measurement by Duro et al. (2011) gives a dimensionless spin parameter[1] of $a = 0.88^{+0.07}_{-0.11}$. Recent results using the continuum fitting method have been obtained by Gou et al. (2011). They find a near-extreme black hole with $a > 0.95$. The work relies on accurate optical determinations of the mass ($14.8 \pm 0.1\,M_{\odot}$) and inclination ($27^{\circ} \pm 0.^{\circ}8$) obtained by Orosz et al. (2011).

Here we study the reflection/iron line approach in detail, taking account of the relativistic effects on the emissivity profile expected if

⋆E-mail: acf@ast.cam.ac.uk

[1] The dimensionless spin parameter $a = cJ/GM^2$, where J and M are the angular momentum and mass of the black hole, respectively.

the black hole spins rapidly. Such effects demand that the emissivity be steep if the disc extends to the innermost region within $\sim 2r_g$ (Wilkins & Fabian 2011). We find $a = 0.97^{+0.014}_{-0.02}$, which is higher than, but marginally consistent with, that reported by Duro et al. (2011). Both reflection results are consistent with the continuum fitting result of Gou et al. (2011).

We find the disc to be fairly highly ionized with an ionization parameter around 1800 erg cm s^{-1}, which means that the reflection spectrum is dominated by a large edge due to ionized iron. This blurred edge carries information about spin in the spectral fit. Early work emphasized how this edge can be important in fitting the spectrum of Cyg X-1 (Ross, Fabian & Brandt 1996).

2 SPECTRAL FITS

The data set we use is one of the 20 *Suzaku* observations of Cyg X-1 analysed by Miller et al. (2012; the observation of 2009 April 8). The focus of that work is not on measuring the black hole spin, but rather on studying the detailed disc–jet coupling in Cyg X-1. The spectra in that work have been fitted with a relativistically blurred reflection model, but in order to make the work tractable, the fits kept the source inclination and iron abundance frozen at 27° and 1, respectively. The emissivity profile of the blurring function was also just a single power law, fixed for the Newtonian value of 3. We relax these assumptions here and apply them to an average data set. We later tested the model on several other data sets (2009 May 6 and 25, and December 1) and obtained consistent results.

The best fit to the 1–500 keV spectrum is shown in Fig. 1, and values of key parameters are given in Table 1. The model used, CONSTANT*TBABS*MTABLE(WINDABS.FITS)(GAUSSIAN +GAUSSIAN +DISKPBB+POWERLAW+KDBLUR2F* ATABLE(EXTENDX.MOD)) HIGHECUT, is shown in Fig. 2. KDBLUR2F is a fast adaptation by Jeremy Sanders of the broken power-law emissivity convolver KDBLUR2. EXTENDX is a version of the self-consistent slab reflection model REFLIONX (Ross & Fabian 2005) extended to allow the photon index to be less than 1.4. (We do not use the REFHIDEN models of Ross & Fabian 2007, which incorporate a blackbody component because they are only available for solar abundance iron and at the blackbody temperature found here for the low state of about 0.16 keV the differences are minimal.) Absorption features due to the stellar

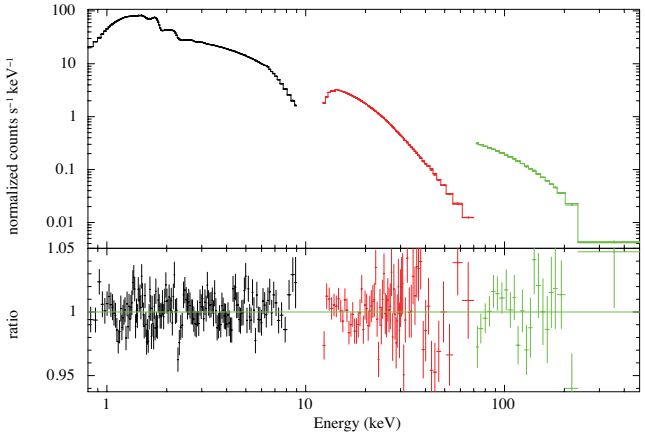

Figure 1. Spectrum of Cyg X-1 in the *Suzaku* XIS0+XIS3 (black), PIN (red) and GSO (green) detectors, from Miller et al. (2012). The ratio to the best-fitting model (Table 1) is shown in the lower panel. The data have been rebinned for display purposes only.

Table 1. Values of key model parameters used in the spectral fitting.

Component	Parameter	Value	q fixed
POWERLAW	Photon index, Γ	$1.37^{+0.014}_{-0.011}$	$1.39^{+0.015}_{-0.009}$
KDBLUR	Inclination (°)	$23.7^{+6.7}_{-5.4}$	$39.8^{+3.0}_{-4.2}$
	R_{in} (r_g)	$1.60^{+0.01}_{-0.16}$	<1.66
	Index, q_1	>6.8	3
	Index, q_2	2.75 ± 0.15	3
	R_{break} (r_g)	4.0 ± 1.1	
REFLIONX	Iron abundance/solar	$1.42^{+0.64}_{-0.15}$	0.89 ± 0.12
	Ionization parameter, ξ erg cm s^{-1}	1765^{+245}_{-178}	2960^{+202}_{-376}
	χ^2/d.o.f.	2217/2419	2411/2421

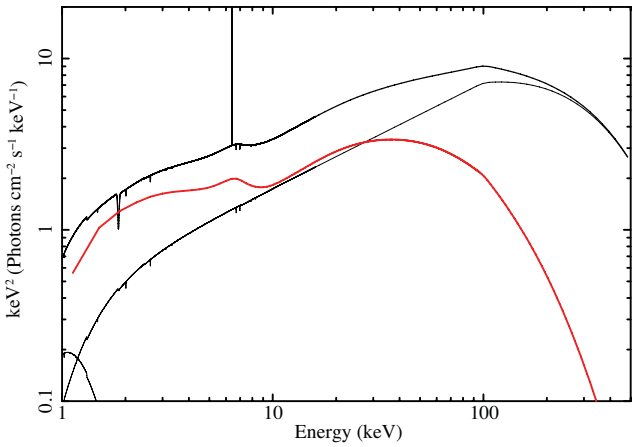

Figure 2. Best-fitting spectral model plotted as EF_E. The relativistically blurred reflection component is shown as the red curve. The 100-keV kink introduced by HIGHECUT has no effect on our spin results.

wind of the companion (e.g. Hanke et al. 2009; Nowak et al. 2011) are modelled using WINDABS.FITS (Miller et al. 2012), and we refer to the last paper for further details. The absorption has little effect on our results. We note that the HIGHECUT model used to fit the data above 100 keV is phenomenological and is not strictly consistent with the 300-keV exponential cut-off assumed by the EXTENDX model, but has limited effect on the results presented here. The quality of the fit is very good, and the emissivity index q is found to be high >6.8. The inclination of $23.^{\circ}7^{+6.7}_{-5.4}$ is consistent with the optical measurement of Orosz et al. (2011).

It is clear that the spectrum is reflection dominated below 10 keV (Fig. 2), although the whole source, from an energy point of view integrating over the whole spectrum, is not reflection dominated. This is a consequence of the hard irradiating continuum where much of the energy absorbed from Compton recoil due to photons at $\sim$100 keV is emitted by the surface layers if the disc is below 6 keV. The ratio of the 0.1–1000 keV flux from the reflection component is 0.70 times that from the power-law component, so the reflection fraction, calculated as the ratio of incident to emitted flux at the disc surface, $\mathcal{R} = 0.7$. The blackbody disc component is 0.4 times the power law, and if reflection is responsible for some of that emission, then $\mathcal{R} \sim 1$. A narrow emission line is introduced at 6.4 keV to account for (weak) distant reflection (e.g. from the stellar companion) and a narrow absorption feature is included at 1.85 keV to compensate for problems in the model response near the detector silicon edge.

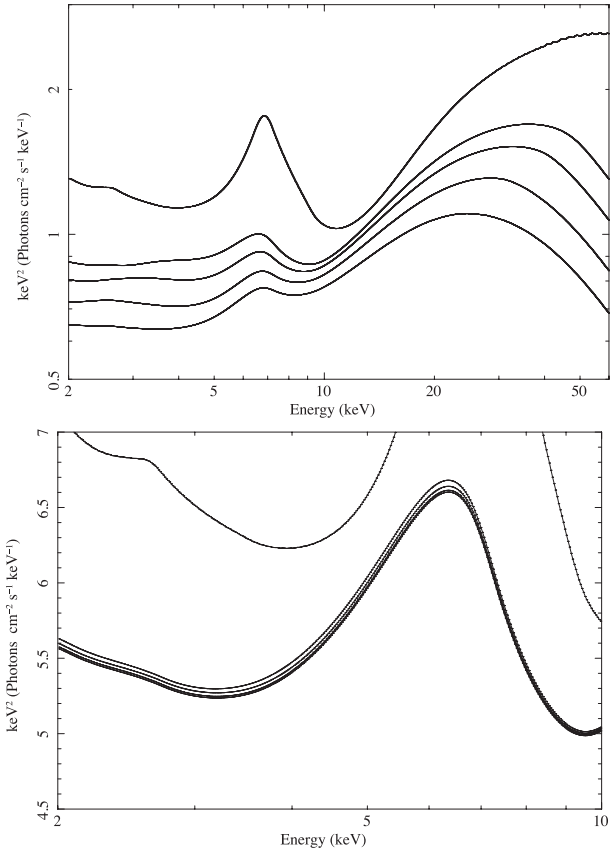

Figure 3. Top: model reflection spectra, relativistically blurred for inner radii of 1.3, 1.5, 1.7, 1.9 and 400r_g with an emissivity index q of 9. Bottom: similar to above, but with $q = 3$ and expanded scales. Note the reduced sensitivity to small values of r_{in}.

We show the model spectrum over the 2–65 keV band in the top panel of Fig. 3. The inner radius has been stepped from 1.3 to 1.9, and then to 400r_g and the innermost emissivity index $q = 9$. The effect of fixing q at 3 is shown in the lower panel: the model is now less sensitive to the innermost radii.

We next fit the spectrum with a model in which the blurring is carried out on many small contiguous annuli, simultaneously. This is similar to the approach taken by Wilkins & Fabian (2011) for the type 1 Seyfert galaxy 1H 0707−495. Once again, the emissivity has a steep index at small radii before breaking to a flatter part, then dropping further close to the Newtonian expected value of 3. Simulations produced by ray tracing in the strong gravity regime revealed in Wilkins & Fabian (2012) show that this triple power-law shape is expected from an irradiated disc around a rapidly spinning black hole. The outer break suggests that the height of the irradiating source above the disc is around 5–7r_g. The results show that emission from within 2r_g is definitely required.

The model which was used to fit the data from the XIS, PIN and GSO simultaneously uses KDBLUR2F, which is a broken power law capturing the essence of Fig. 4. We investigated the dependence of the inner radius r_{in} on various key parameters, the iron abundance and the inclination (Figs 5–7).

The data require an iron abundance which is slightly supersolar, an inclination less than ∼30° and an intermediate-ionization parameter around 1760. All results strongly point to an inner radius less than 2r_g, even if q is fixed at 3 (Table 1, Fig. 7).

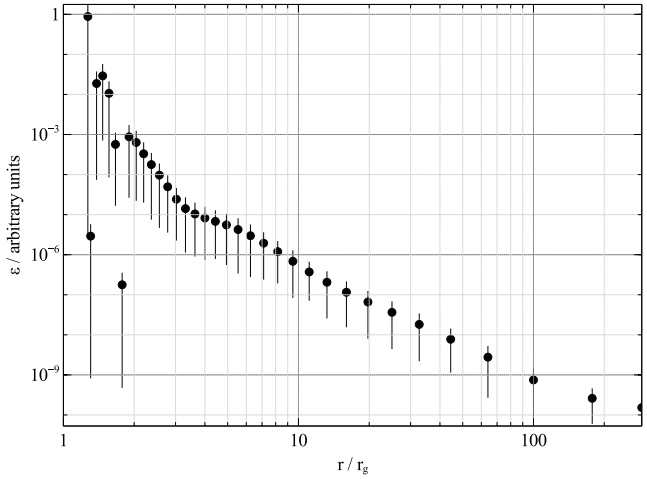

Figure 4. Emissivity profile obtained by fitting the blurred reflection model to small increments in radius. The profile has the characteristic steep–flat–moderate profile expected from irradiation by a source at a height $h = 5$–$7r_g$ above the black hole. The innermost annulus with a significant detection is at $r \sim 1.4r_g$.

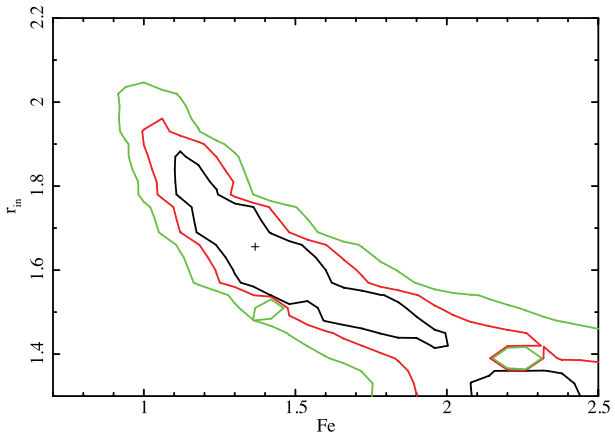

Figure 5. Effect of varying the inner radius r_{in} as a function of iron abundance Fe.

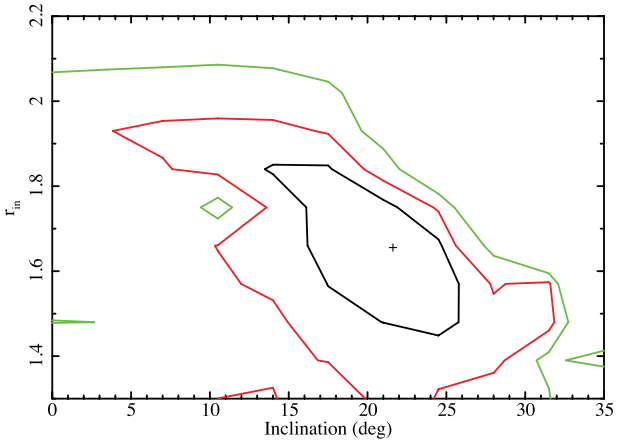

Figure 6. Effect of inclination on inner radius r_{in}.

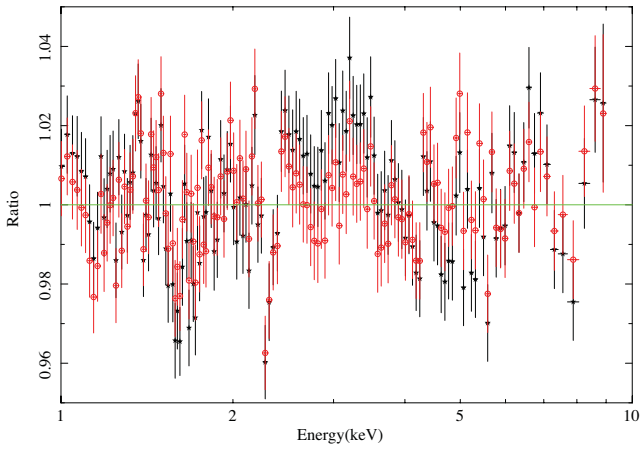

Figure 7. Ratio of (heavily binned) spectral data points to the best-fitting model with a single power-law emissivity profile (index q fixed at 3: black points) and to the broken power-law model with variable indices (red points).

As a test, we have fitted the PIN data alone, since this data set is sensitive to the reflection hump. The iron abundance is fixed at unity (the depth of the edge in the XIS data indicates that the abundance cannot be either very low or very high). We also fix the inclination at 27°, obtaining again $r_{\rm in} < 2r_{\rm g}$. This confirms that fitting the reflection hump alone can in principle measure spin.

The reflection fits presented here all strongly point to the spin of the black hole being high. Using the broken power-law emissivity model RELCONVF (a faster modification by JSS of RELCONV of Dauser et al. 2010, 2012) yields $a = 0.97^{+0.014}_{-0.02}$ at the 90 per cent confidence level. The results for the other parameters are similar to those shown in Table 1.

We have also used the Novikov & Thorne (1973; see also Page & Thorne 1974) emissivity profile which is appropriate if the corona is immediately above the disc. The emission then varies with radius in the manner expected from a radiatively efficient thin disc. The resulting fit has $\chi^2 = 2422/2422$, significantly worse than the earlier best fit. High spin ($a > 0.98$) is again required and the inclination is higher ($i \sim 39°$).

2.1 The Newtonian power-law emissivity profile, $q = 3$

Duro et al. (2011) measure the broad iron line of Cygnus X-1 as seen by *XMM–Newton* in the EPIC-pn modified timing mode. They report that the black hole is spinning close to maximal with value $a = 0.88^{+0.07}_{-0.11}$, on adopting the Newtonian, single power-law emissivity profile with index fixed at $q = 3$. A fit with q free gave $q = 10^{+0}_{-6}$ and $a = -0.1 \pm 0.4$. They rightly dismiss the statistically more probable, high q low spin, solution as making no physical sense, since high q is only applicable at high spin.

Fitting our spectra with q fixed at 3 leads to a much worse (although acceptable) fit with $\Delta\chi^2 = +194$ (Table 1). The inner radius is inferred to be at less than $1.66r_{\rm g}$, the inclination is above 35° (which is inconsistent with the optical result) and the ionization parameter is higher at nearly 3000. If the inclination is fixed at 25°, then $r_{\rm in} < 1.9r_{\rm g}$. The conclusion that the black hole is rapidly spinning remains robust.

The spectral residuals obtained from using a single fixed value of q and a broken power law with variable indices are shown in Fig. 7. The large difference in χ^2 is mostly due to the red wing of the line feature at 2.5–3.5 keV and (to a much lesser extent) the edge at 6.5–7.5 keV. The residuals for fixed q are at about 2 per cent and increase to 3 per cent or more if $r_{\rm in}$ is increased to $3r_{\rm g}$ and beyond. This demonstrates where our information is coming from and shows that from a statistical point of view we can probe the strong gravity regime.

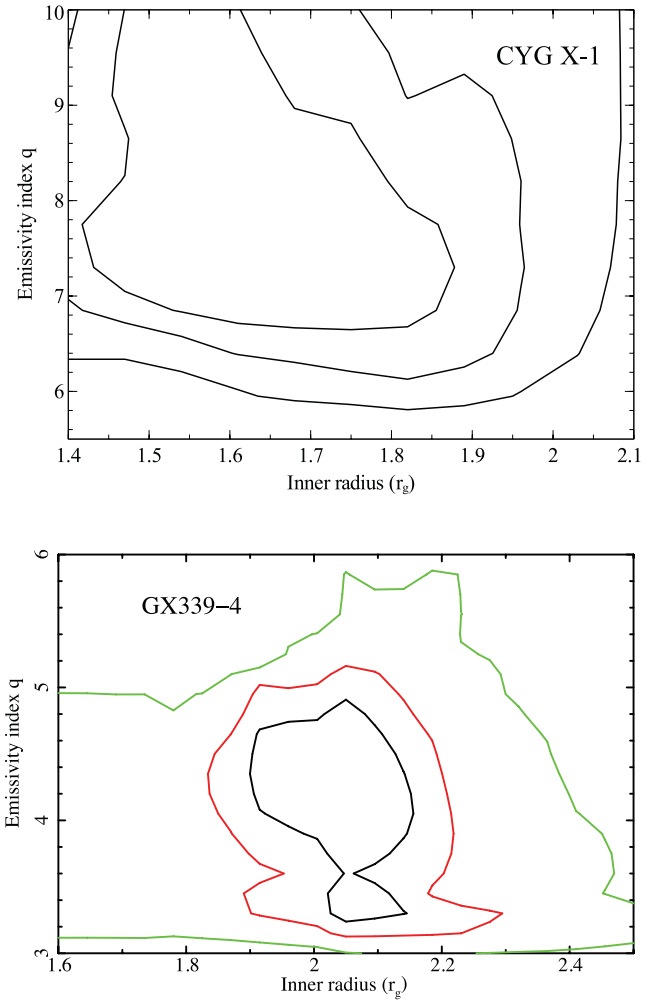

Figure 8. Variation of inner emissivity index q_1 on inner radius $r_{\rm in}$ for Cyg X-1 (top) and GX 339−4 (bottom). A broken power-law emissivity profile is used with the outer index, q_2, fixed at 3, for both plots.

A single power-law emissivity has only limited validity. It is clear from the fitted emissivity profile in Fig. 4 that a slope of 3 is a fair approximation from $r = 2r_{\rm g}$ outwards. It underestimates the profile within $r = 2r_{\rm g}$ and is therefore a poorer probe of the innermost region (see Fig. 3). If $q = 3$ is used, then it will likely yield an upper limit to the inner radius and thus a lower limit on the spin. Doubly broken power-law profiles are required when fitting for the inner radius and/or spin when the spin is high ($r_{\rm in} < 2r_{\rm g}$ and $a > 0.94$).

Cyg X-1 is a good example where a steep inner profile is needed (Fig. 8). In contrast, the source GX 339−4, which has an inner radius of $\sim 2r_{\rm g}$ and thus moderate spin, requires only a mildly steep index q of around 4 (Fig. 7). [We use the *XMM* data of the low-state observation of GX 339−4 from Reis et al. (2008) for this figure.]

The higher state of Cyg X-1 during the Duro et al. (2011) observations, in which the blackbody component contributes to about 3 keV, may complicate variable q measurements.

3 MODIFICATIONS TO ALLOW FOR THE TIME VARIABILITY OF Cyg X-1

In this section we consider what modifications can be made to the spectral model developed here to allow for the complex time variability observed in Cyg X-1. The aim is not to build a complete model which accounts for everything that has been observed but to indicate the directions in which modifications are needed.

Study of the rapid variability of Cyg X-1 requires high count rates and thus instruments with large collecting areas, such as *EXOSAT* (Belloni & Hasinger 1990), *Ginga* (Miyamoto et al. 1988; Miyamoto & Kitamoto 1989; Gierliński et al. 1997) and *RXTE* (Nowak et al. 1999; Revnivtsev, Gilfanov & Churazov 1999; Gilfanov, Churazov & Revnivtsev 2000; Pottschmidt et al. 2003). The power spectrum is flat up to about 0.02 Hz, above which it drops with frequency f as f^{-1} up to a few Hz where it steepens to f^{-2}. Time lags are seen over the frequency range 0.1–30 Hz in which soft bands lead hard bands, with the longest time lags being 0.05 s. As a light crossing time, this corresponds to a distance of $\sim 1000 r_g$, which is much larger than the radius of any of the regions inferred by our spectral fitting. The lag time-scale must therefore be some form of propagation time. In the low state, such as observed here, the iron 'line' is found to be variable up to a frequency of a few Hz (Revnivtsev et al. 1999). This is too low a frequency to be compatible with any light crossing time effects expected in our spectral model.

Several models have been made for the spectral variability and time lags. Some early models are reviewed by Poutanen (2001). A model by Lyubarskii (1997) in which fluctuations are generated by and propagate inwards through the disc has been extended by Arévalo & Uttley (2006) to explain many of the features observed. Most recently the hard state lags have been modelled as propagating oscillations in a hot inner flow in the central region of an accretion disc truncated at about $20 r_g$ (Kawabata & Mineshige 2010), prompted by results of an earlier *Suzaku* observation of Cyg X-1 reported by Makishima et al. (2008). In that work the corona was modelled as having two optical depths, which allow for softer and harder continua. Reflection was dealt with by a phenomenological model involving cold unblurred reflection and a broad Gaussian iron line.

The results obtained from the fits presented here reveal an inner radius of less than $2 r_g$ strongly irradiated by a corona situated at ~ 5–$7 r_g$. This is incompatible with an extensive inner corona. The single power-law continuum used here does not allow for time lags unless it varies in slope on the required time-scales. To allow for slope variations we have fitted the spectrum with two power-law continua, the steeper of which gives rise to the reflection. The spectral fitting is degenerate provided that the sum of the two power laws approximates the single power law shown in Fig. 2. For illustration purposes we have selected a pair of spectral indices which give a good fit (Fig. 9; Table 2). Reflection continues to dominate the spectrum below 10 keV.

A simple physical interpretation arises if the source of the steeper power law is quasi-static and situated close to the centre of the disc, therefore producing the reflection. The harder component could originate from further out within the moving jet; both soft source photons from the disc and reflection produced by the continuum are reduced by beaming (Beloborodov 1999). Time lags then occur if variations propagate up the jet from the inner, quasi-static and softer component to the outer, jetted harder component. They need not propagate at jet speed, but could be due to changes in the magnetic structure or collimation of the jet. The power in these components and the jet is presumed to derive from the accretion disc and be transferred by magnetic fields coupled to a range of radii, so varying in a manner which is consistent with the Lyubarskii model.

The lack of rapid reflection variations reported by Revnivtsev et al. (1999) could in part be due to light bending effects implicit in the proximity of the inner, softer, power-law component to the black hole (Miniutti & Fabian 2004), if some of the rapid variability is due to (small) changes in the height of that inner component.

Further development of such models is beyond the scope of this paper, which is focused on the low-state X-ray spectrum of Cyg X-1.

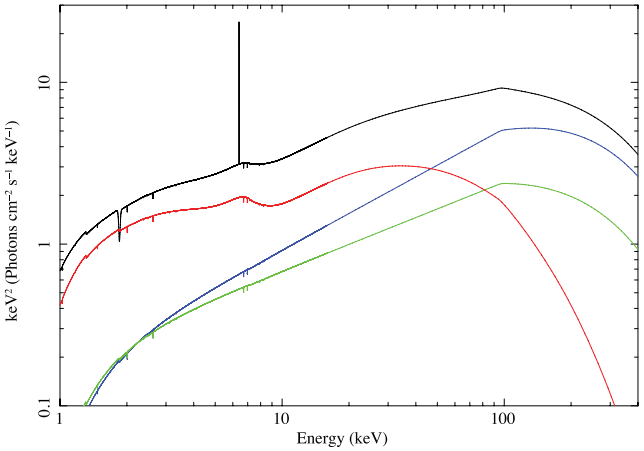

Figure 9. Model spectrum with two power-law components. The index of the incident spectrum for the reflection component equals that of the steeper power law.

Table 2. Values of model parameters obtained from the best fit with two power-law components of spectral indices Γ_s and Γ_h. The incident spectrum for the reflection has index Γ_s.

Component	Parameter	Value
POWERLAW	Photon index, Γ_s	1.45*f*
POWERLAW	Photon index, Γ_h	1.25*f*
	R_{in} (r_g)	1.63
REFLIONX	Iron abundance/solar	1.28
	Ionization parameter, ξ erg cm s^{-1}	1775
	χ^2/d.o.f.	2219/2419

4 DISCUSSION

We have used the X-ray reflection fitting method to obtain a robust measurement of the dimensionless spin parameter of the black hole in Cyg X-1 of $a = 0.97^{+0.014}_{-0.02}$. Our result agrees with the continuum fitting value of Gou et al. (2011) and yields an even higher spin than the reflection measurement of Duro et al. (2011). Cygnus X-1 definitely appears to have high spin.

We argue that non-Newtonian values must be used for the inner emissivity profile of the reflected emission of the innermost disc when the spin is high ($r_{\rm in} < 2r_{\rm g}$ and $a > 0.94$).

The reflection fitting method relies on detection of the innermost radius of the disc which is dense enough for reflection to occur. We assume that this is the ISCO, for within that radius the plunge orbits mean that the gas density drops rapidly so the reflection signal vanishes. Although magnetic fields may have some effect here, we consider it reasonable to assume that the dense parts of the disc that give the reflection spectrum are not seriously affected (see discussion and simulations in Reynolds & Fabian 2008; Shafee et al. 2008). There is nevertheless a systematic uncertainty here which simulations need to resolve.

The reflection fraction $\mathcal{R} \sim 0.7$ is low compared with the simple expectation of a source close to the black hole at $h \sim 5r_{\rm g}$. Light bending should give $\mathcal{R} \sim 2$ (e.g. Fabian et al. 2011). The observed radio emission (Miller et al. 2012) means that a jet is operating, so it is plausible that the emission model is more complex, as discussed in Section 3. We suggest there that irradiation of the disc by the quasi-static base of the jet at a 5–7$r_{\rm g}$ gravitational radii is responsible for the reflected emission, whereas the observed power-law continuum is dominated by higher, faster parts of the jet which mildly beam emission in our direction.

Systematic uncertainties in the models and (relative) spectral calibration can also affect the details of our fits and thus results, particularly of the innermost region. The continuum fitting method is also subject to systematic uncertainties in both models and spectral calibration (relative and absolute).

Wide agreement on the high spin of Cygnus X-1 boosts confidence in spin measurements from the reflection fitting method of other objects as well as AGN, where it is the only method yet available.

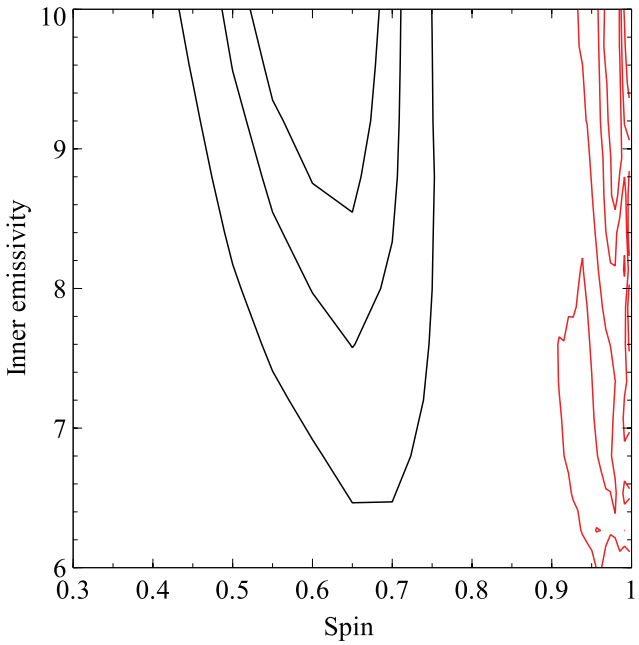

Figure 10. Emissivity–spin contours for (left, black) a simple power-law profile and (right, red) a broken power-law profile with the outer index fixed at 3. The minimum χ^2 for the fit using the broken power law is about 150 below that for the fit using a single power-law emissivity profile. The results in Table 1 were obtained with the outer index free.

The spectral fits strongly indicate that the innermost radius of the disc lies within $2r_{\rm g}$. Relativistic effects are strong there and a simple Newtonian assumption for the emissivity profile is inappropriate. The effects are inescapable and involve both special relativity, since the velocity of the reflecting matter on the disc is high, and general relativity, through gravitational redshift and light bending (Wilkins & Fabian 2011, 2012).

Theoretical emissivity profiles due to point sources at different heights on the rotation axis above the disc plane are shown in fig. 12 of Fabian et al. (2011). When the source height exceeds $3r_{\rm g}$, the emissivity profile breaks at radius $r \sim h$ to the Newtonian value of 3 outside and flatter within. The inner profile rapidly steepens to a high value within $2r_{\rm g}$, if the disc extends in that far.

We recommend that $q = 3$ be used initially. Should this lead to high spin being suspected, then a power law broken at least once, with a high inner index ($q_1 > 3$), should be used. This is illustrated in Fig. 10 where we have fitted our Cyg X-1 data by a single power-law emissivity of free index. It shows the best fit being of high index and relatively low spin ($q \sim 10, a \sim 0.6$), which is rejected by the physical sense argument of Duro et al. (2011). If instead we use a broken power-law emissivity fixing the outer index $q_2 = 3$, then we find that the inner emissivity q_1 remains high and the spin rises to be very close to maximal ($a > 0.95$). This now makes physical sense. Allowing the outer index to be free gives the results of Table 1.

ACKNOWLEDGMENTS

We thank the referee for comments leading to Section 3. ACF thanks the Royal Society for support. RCR thanks the Michigan Society of Fellows and NASA for support through the Einstein Fellowship Programme, grant number PF1-120087.

REFERENCES

Arévalo P., Uttley P., 2006, MNRAS, 367, 801
Belloni T., Hasinger G., 1990, A&A, 227, L33
Beloborodov A. M., 1999, ApJ, 510, 123
Dauser T., Wilms J., Reynolds C. S., Brenneman L. W., 2010, MNRAS, 409, 1534
Dauser T. et al., 2012, MNRAS, 422, 1914
Duro R. et al., 2011, A&A, 533, L3
Fabian A. C. et al., 2011, MNRAS, 419, 116
Gierliński M. et al., 1997, MNRAS, 288, 958
Gilfanov M., Churazov E., Revnivtsev M., 2000, MNRAS, 316, 923
Gou L. et al., 2011, ApJ, 742, 85
Hanke M., Wilms J., Nowak M. A., Pottschmidt K., Schulz N. S., Lee J. C., 2009, ApJ, 690, 330
Kawabata R., Mineshige S., 2010, PASJ, 62, 621
Lyubarskii Y., 1997, MNRAS, 292, 679
Makishima K. et al., 2008, PASJ, 60, 585
Miller J. M., Wojdowski P., Schulz N. S., Marshall H. L., Fabian A. C., Remillard R. A., Wijnands R., Lewin W. H. G., 2005, ApJ, 620, 398
Miller J. M., Reynolds C. S., Fabian A. C., Miniutti G., Gallo L. C., 2009, ApJ, 697, 900
Miller J. M., Pooley G. G., Fabian A. C., Nowak M. A., Reis R. C., Cackett E. M., Pottschmidt K., Wilms J., 2012, ApJ, submitted
Miniutti G., Fabian A. C., 2004, MNRAS, 349, 1435
Miyamoto S., Kitamoto S., 1989, Nat, 342, 773
Miyamoto S., Kitamoto S., Mitsuda K., Dotani T., 1988, Nat, 336, 450
Novikov I. D., Thorne K. S., 1973, in DeWitt C., DeWitt B., eds, Black Holes. Gordon & Breach, New York
Nowak M. A., Vaughan B., Wilms J., Dove J. B., Begeman M. C., 1999, ApJ, 510, 874
Nowak M. A. et al., 2011, ApJ, 728, 13

Orosz J. A., McClintock J. E., Aufdenberg J. P., Remillard R. A., Reid M. J., Narayan R., Gou L., 2011, ApJ, 742, 84
Page D. N., Thorne K. S., 1974, ApJ, 191, 499
Pottschmidt K. et al., 2003, A&A, 407, 1039
Poutanen J., 2001, Advances Space Res., 28, 267
Reis R. C., Fabian A. C., Ross R. R., Miniutti G., Miller J. M., Reynolds C. S., 2008, MNRAS, 387, 1489
Revnivtsev M., Gilfanov M., Churazov E., 1999, A&A, 347, L23
Reynolds C. S., Fabian A. C., 2008, ApJ, 675, 1048
Ross R. R., Fabian A. C., 2005, MNRAS, 358, 211
Ross R. R., Fabian A. C., 2007, MNRAS, 381, 1697
Ross R. R., Fabian A. C., Brandt W. N., 1996, MNRAS, 278, 1082
Shafee R., McKinney J. C., Narayan R., Tcekhovsky A., Gammie C. F., McClintock J. E., 2008, ApJ, 687, L25
Wilkins D. R., Fabian A. C., 2011, MNRAS, 414, 1269
Wilkins D. R., Fabian A. C., 2012, MNRAS, in press

This paper has been typeset from a TEX/LATEX file prepared by the author.